

Modulations in the Oscillatory Activity of the Globus Pallidus internus neurons during a Behavioral Task-A Point Process Analysis

Shreya Saxena*, John T. Gale[†], Emad N. Eskandar[‡] and Sridevi V. Sarma*

* Department of Biomedical Engineering, Johns Hopkins University

[†] Department of Neurosciences, Cleveland Clinic

[‡] Department of Neurosurgery, Harvard Medical School

Abstract—The behavioral state of a subject is hypothesized to be reflected in the oscillatory modulations of the spiking activity of certain groups of neurons. In particular, the beta- and gamma-bands have been experimentally shown to be related to movement in the motor cortex and parts of the basal ganglia. Here, we analyze the relationship between directional tuning and oscillations in the beta- and gamma-bands of the neurons in the Globus Pallidus internus (GPi) of two healthy nonhuman primates during a radial center-out motor task. We find that, during the planning stages of the movement, the percentage of directionally tuned neurons displaying gamma oscillations increases when compared to the percentage of directionally tuned neurons displaying beta oscillations. A similar trend is not seen in non-directionally tuned neurons. This suggests that the GPi neurons involved in the planning of movement communicate information using an emergence of oscillations in the gamma-band.

I. INTRODUCTION

Neurons carry information and communicate with each other through oscillatory modulations in spiking activity during task related events. For example, theta-band (4–7 Hz) oscillations are observed in the hippocampus during its ‘online’ state [1], and alpha-band (6–12 Hz) oscillations are seen in the cortex during a period of relaxation when the eyes are closed [2]. Beta-band (15–30 Hz) and gamma-band (30–80 Hz) oscillations are hypothesized to communicate movement-related events in motor structures of the brain.

The presence of beta-band oscillations has been observed at rest in motor areas, combined with a suppression of these oscillations during movement. This phenomenon has been observed in the striatum of the healthy monkey [3], the healthy human putamen [4] and cortex [5]–[9], as well as the Parkinsonian subthalamic nucleus [10]. Gamma-band activity in the motor cortex has been observed to be more prevalent in the planning phase of a movement, and has been observed to decrease thereafter [11]–[13]. The simultaneous occurrence of the suppression of beta-band activity and an increase in gamma-band activity in the same trial (a “cross over” effect) has been reported in the sensorimotor cortex during movement [7], [8]. In this study, we investigate whether the GPi neurons display a similar cross over effect in beta- and gamma- band activity.

Directional tuning is traditionally analyzed by comparing firing rates of the same neuron when the subject moves in different directions [14]. The power contained in a specific frequency band is computed either using local field potential

data, which is not neuron-specific, or using the power spectra of the activity of the neurons in question. Traditionally the two statistics, i.e. directional tuning and power in a frequency band, are calculated by manipulating the data using first and second-order statistics of the spike trains respectively.

We propose modeling the activity of the GPi neurons taking into account the point process nature of the spiking activity of the neurons [15]. Point process methods have been used to analyze systems of neurons in many previous studies [10], [15]–[17]. A single point process model (PPM) captures the directional tuning as well as the oscillations of that neuron for different ranges of frequencies, thus eliminating the need for several manipulations of the spike trains [10].

In this paper, we study oscillatory dynamics in the spiking activity of GPi neurons recorded from a nonhuman primate executing a radial center-out task. We first use PPMs to characterize the spiking dynamics of individual neurons and use the model parameters to identify directionally tuned neurons. These comprise a subset of the population that display significantly different firing properties while the primate is reaching in a direction. We then examine the oscillatory activity in the beta and gamma bands of all neurons for each trial type using the PPM model parameters, and analyze the differences between the two subpopulations of GPi neurons : directionally tuned vs. non-directionally tuned neurons.

We found that the percentage of non-directionally tuned neurons having activity in the beta- and gamma-bands does not change significantly during movement. However, a higher percentage of directionally tuned neurons are seen to display oscillations in the gamma-band as compared to the beta-band during the planning of movement, which is when the GPi neurons are hypothesized to be involved in motor behavior. Thus, it can be inferred that the GPi neurons involved in the planning of movement communicate information using an emergence of oscillations in the gamma-band.

II. METHODS

A. Experimental Procedures

Two normal non-human primates were trained to perform a radial center-out motor task. Each trial began with the onset of a fixation point at the center of a screen. To initiate a trial, the animals were required to fixate on a central fixation point for a period of 400–800 ms. Breaking fixation immediately aborted the trial without any liquid reward. At this point, eight

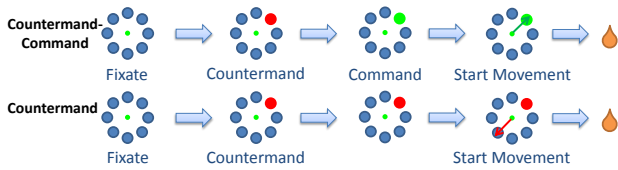


Fig. 1. Trial Types

gray objects appeared in a radial arrangement equidistant from the center of the screen. While maintaining gaze on the fixation point, a random gray target was replaced by a stimulus cue.

There were four trial types, described below. In the Command trial type, a random gray target was replaced by a green stimulus cue. In the Command-Countermand trial type, a random gray target was replaced by a green stimulus cue. After a delay of up to 1000 ms, the same target was replaced by a red stimulus cue. In the Countermand-Command trial type, a random gray target was replaced by a red stimulus cue. After a delay of up to 1000 ms, the same target was replaced by a green stimulus cue. In the Countermand trial type, a random gray target was replaced by a red stimulus cue. In the Command and Countermand-Command trial types, the primate was required to make a joystick movement in the direction of the target since it was cued with a final green light. In the Countermand and Command-Countermand trial types, the primate moved to the 180° radially opposite direction of the target since it was cued with a final red light. The trial was concluded when the primate reached the target in the desired direction, and a liquid reward was administered. Target positions and trial types were randomized such that many movements toward each of the eight positions could be analyzed over the course of a single recording session.

Of all the trial types, here we present the analysis results from two of the trial types, i.e. the Countermand-Command and Countermand trial types to be able to analyze the effect of the initial red cue in greater detail. These two trial types are summarized in Fig. 1.

While the primates were performing the behavioral task, extracellular microelectrode recordings were made from the GPI. An off-line computer algorithm (Offline-Sorter, Plexon Inc., Houston, TX) removed stimulus artifacts and discriminated individual neurons simultaneously recorded in the multi-unit raw microelectrode signal. $n = 27$ neurons were recorded from the GPI of the first primate, and $n = 56$ from the GPI of the second primate.

B. Point Process Models

A point process is a series of 0-1 random events that occur on a continuum such as space or time. For a neural spike train, the 1s are individual spike times and the 0s are the times at which no spikes occur. To define a PPM of neural spiking activity, we consider an observation interval $(0, T]$ and let $N(t)$ be the number of spikes counted in interval $(0, t]$ for $t \in (0, T]$. A point process model of a neural spike train can then be completely characterized by its conditional

intensity function (CIF), defined as

$$\lambda(t|H_t) \triangleq \lim_{\Delta \rightarrow 0} \frac{\Pr(N(t + \Delta) - N(t) = 1|H_t)}{\Delta}, \quad (1)$$

where H_t denotes the spiking history up to time t . It follows from (1) that the probability of a single spike in a small interval $(t, t + \Delta]$ is approximately $\lambda(t|H_t)\Delta$. Details can be found in [18]. The CIF generalizes the rate function of a Poisson process to a rate function that is history dependent. Because the CIF completely characterizes a spike train, defining a model for the CIF defines a model for the spike train [19]. For our analyses, we use the generalized linear model (GLM) to define our CIF models by expressing for each neuron, the log of its CIF in terms of the neuron's own spiking history and relevant movement covariates [20]. We compute model parameters from the data via maximum likelihood estimation [19].

We express the CIF for each neuron as a function of movement direction $\{1, 2, \dots, 8\}$, which correspond to 0, 45, 90, ..., 315 degrees clockwise from the 'Up' direction. Instead of estimating the CIF continuously throughout the entire trial, we estimate it over 400 ms time windows around key epochs and at discrete time intervals each 1 ms in duration. At each epoch, we express the CIF as

$$\lambda(t|H_t, \Theta) = \lambda^S(t|\Theta) \cdot \lambda^H(t|H_t, \Theta), \quad (2)$$

where $\lambda^S(t|\Theta)$ describes the effect of the movement direction stimulus on the neural response and $\lambda^H(t|H_t, \Theta)$ describes the effect of spiking history on the neural response. Θ is a parameter vector to be estimated from data.

We assessed the goodness-of-fit of each PPM (2) on the validation data (cross-validation) with the Kolmogorov-Smirnov (KS) plot after time rescaling of the spike trains [10], [16], [19], [21]. We computed the 95% confidence bounds for the degree of agreement using the distribution of the KS statistic [21] and included in our analysis only those PPMs whose KS plots visually displayed a high goodness-of-fit.

C. Directional Tuning

The PPMs were used to determine directional tuning of each neuron. We first define the model structure used to characterize the firing activity of the neurons. We express the CIF as in (2), and model the history-independent parameters using the following GLM structure for λ^S , for $d = \{1, 2, \dots, 8\}$.

$$\log \lambda^S(t|\alpha, d) = \alpha_d \quad (3)$$

For all PPMs, the history-dependent parameters are modeled in the following manner.

$$\begin{aligned} \log \lambda^H(t|\phi, \beta, \gamma) = & \sum_{j=0}^9 \phi_j n(t - j : t - (j + 1)) \\ & + \sum_{k=0}^9 \gamma_k n(t - (2k + 10) : t - (2k + 12)) \\ & + \sum_{l=0}^8 \beta_l n(t - (5l + 30) : t - (5l + 35)), \end{aligned} \quad (4)$$

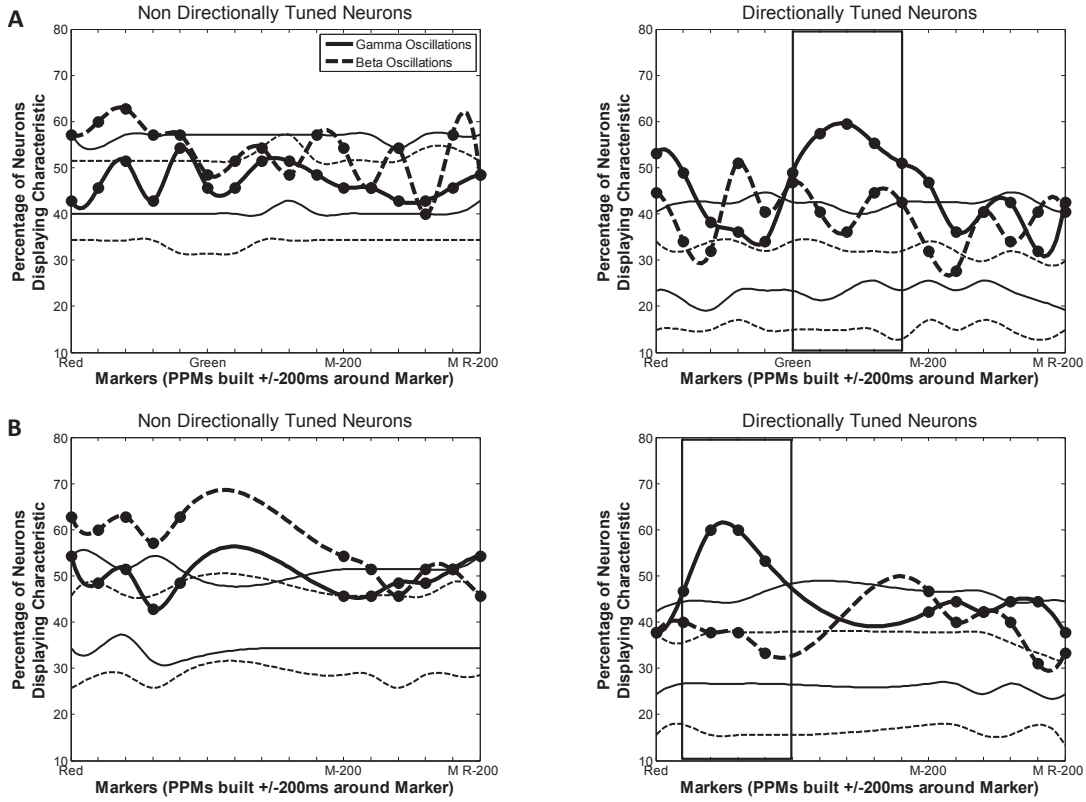


Fig. 2. The percentage of neurons displaying gamma (solid) and beta (dashed) oscillations amongst non-directionally tuned neurons (left) and directionally tuned neurons (right) for trial types A) Countermand-Command, and B) Countermand. The thin lines indicate the 5 and 95% bounds of the distribution of the percentage of neurons displaying gamma (solid) and beta (dashed) oscillations as calculated from spike trains with randomly shuffled interspike intervals. The boxed-in regions indicate the period where a cross over effect occurs, i.e. where the percentage of neurons displaying gamma oscillations is higher as compared to the percentage of neurons displaying beta oscillations.

where $n(a : b)$ is the number of spikes observed in the time interval $[a, b)$ during the epoch. The $\{\phi_j\}_{j=0}^9$ parameters measure the effects of spiking history in the previous 10 ms and therefore can capture refractoriness and / or bursting on the spiking probability in the given epoch [10]. The $\{\gamma_k\}_{k=0}^9$ and the $\{\beta_l\}_{l=0}^8$ parameters are described in more detail in Section II-D.

If the history-independent firing in one direction was found to be significantly different from at least four other directions at a 95% confidence level, the neuron was determined to be directionally tuned. Specifically, for each direction $d' \in 1, 2, \dots, 8$, we computed $p_{d'd} = \Pr(e^{\alpha_{d'}} > e^{\alpha_d}) = \Pr(\alpha_{d'} > \alpha_d)$ for $d \neq d'$. We defined $p_{d'd} = 0$. We used the Gaussian approximation for α_d , which is one of the asymptotic properties of maximum likelihood estimates to compute $p_{d'd}$ [19]. Let $N_d = \#\{d' \in 1, 2, \dots, 8\}$ for which $p_{d'd} \geq 0.975$. If $N_d \geq 4$ for any $d \in 1, 2, \dots, 8$, the neuron was determined to be directionally tuned. For further analyses, different models were constructed for directionally tuned vs. non-directionally tuned neurons, as described below.

1) *Models for Directionally Tuned Neurons*: If the neuron is determined to be directionally tuned using the criteria detailed previously, we constructed a new model for that neuron using only the data from the trials where the primate was reaching in direction d^* , where d^* is the directionally tuned direction. If more than one direction was determined to be tuned in the neuron, then $d^* = \operatorname{argmax}_d(\alpha_d - \operatorname{mean}(\alpha_d))$, $d \in \{1, 2, \dots, 8\}$. The structure for the history-

independent term was now defined as the following.

$$\log \lambda^S(t|\alpha) = \alpha \quad (5)$$

The history-dependent term λ^H remained the same as in (4).

2) *Models for Non Directionally Tuned Neurons*: If the neuron was not directionally tuned in any direction, model structures (3) and (4) remained the same. Note that the history-dependent terms are the same for directionally and non-directionally tuned neurons.

D. Presence of Oscillations

To determine the presence of oscillations in the spiking activity of a neuron, we analyzed the relevant parameters in the parameter vector Θ estimated from data for the PPMs built for each neuron (Sections II-C1 and II-C2).

The parameters $\{\gamma_k\}_{k=0}^9$ measure the effects of spiking history in the previous 10 to 30 ms, and therefore can capture the presence of oscillations in the frequency range of 33 to 100 Hz. This corresponds to the gamma frequency band, and we determined the presence of oscillations in this frequency range if the probability of firing at any one frequency in the range is higher than 1, that is, for at least one $k = 0, \dots, 9$ $LB_k > 1$, where $LB_k \leq e^{\gamma_k}$. LB_k is the 99% lower confidence bound for parameter k .

Similarly, the parameters $\{\beta_l\}_{l=0}^8$ measure the effects of spiking history in the previous 30 to 75 ms, and therefore can capture the presence of oscillations in the frequency range of 13 to 33 Hz. This corresponds to the beta frequency band, and

we deemed oscillations to be present in this frequency range if for at least one $l = 0, \dots, 8$ $LB_l > 1$, where $LB_l \leq e^{\beta l}$. LB_l is the 99% lower confidence bound for parameter l .

III. RESULTS

The data from the trials was divided into different epochs of length 400ms each. The center of these time windows are as follows (in ms): [Red, Red+50, Red+100, Red+150, Red+200, Green, Green+50, Green+100, Green+150, Green+200, M-200, M-150, M-100, M-50, M, Reward-200] for the Countermand-Command trial type, and [Red, Red+50, Red+100, Red+150, Red+200, M-200, M-150, M-100, M-50, M, Reward-200] for the Countermand trial type (M corresponds to Start of Movement and the color to the color of the cue).

For each trial type, we first determined the directionally tuned neurons as those neurons which were directionally tuned in the epoch which had the highest percentage of directionally tuned neurons for that trial type. This epoch had its center at $M - 100$ ms for trial type Countermand-Command, and at $M - 150$ ms for trial type Countermand. Once we had differentiated the directionally tuned neurons from the non-directionally tuned neurons, we determined the percentages of each sub-group of neurons that displayed beta oscillations, and compared this with the percentage that displayed gamma oscillations at each epoch (Fig. 2). We also computed these percentages for randomized spike trains, built by shuffling the interspike intervals of the original spike trains for each trial of each neuron a total of 100 times. The 5 and 95% bounds of these percentages are displayed in thin lines in Fig. 2, the region representing the percentage of neurons in which these oscillations may occur by chance.

We can see that the percentage of directionally tuned neurons displaying oscillations in the gamma frequency band was higher than the percentage of these same neurons displaying oscillations in the beta frequency band during the planning stage of the movement, i.e., after the final cue was displayed. This percentage of neurons is also significant, i.e. is higher than the bounds constructed from randomized spike trains. The same is not true for non-directionally tuned neurons, where the percentage of neurons displaying frequencies in the beta band, also significant, is seen to be slightly higher during most epochs for both trial types.

This suggests that the modulations in the oscillatory activity in the beta and gamma bands of the directionally tuned GPi neurons is at a population level, and is related to the eventual movement of the primates.

IV. CONCLUSIONS

In this study, we use a novel method that takes advantage of the point process nature of the neural spikes to visualize the oscillatory activity of the neurons during different epochs of the tasks. We believe that this method can be used for different systems to assess the relationship between directional tuning and the modulations in the oscillations in different frequency ranges. We can see from these results that the oscillatory activity of the directionally tuned GPi neurons

is modulated towards a higher percentage of GPi neurons displaying significant oscillations in the gamma frequency band rather than the beta frequency band during the planning of movement towards or away from a target given in a specific direction. The presence of this cross over effect in task related neurons suggests that the modulations in the oscillatory activity in the beta- and gamma- bands of the directionally tuned GPi neurons are at a population level, and are related to the eventual movement of the primates.

REFERENCES

- [1] G. Buzsaki, "Theta oscillations in the hippocampus," *Neuron*, vol. 33, pp. 325 – 340, 2002.
- [2] E. Niedermeyer, "The normal EEG of the waking adult," in *Electroencephalography (Niedermeyer, E. and Lopes da Silva, F.)*. Philadelphia: Lippincott Williams & Wilkins, 2005, ch. 9, pp. 167–192.
- [3] R. Courtemanche, N. Fujii, and A. M. Graybiel, "Synchronous, focally modulated β -band oscillations characterize local field potential activity in the striatum of awake behaving monkeys," *J Neurosci*, vol. 23, no. 37, pp. 11 741–11 752, 2003.
- [4] D. Sochurkova and I. Rektor, "Event-related desynchronization/synchronization in the putamen. an SEEG case study," *Exp Brain Res*, vol. 149, pp. 401–404, 2003.
- [5] M. Alegre, et al., "Beta EEG changes during passive movements: sensory afferences contribute to beta event-related desynchronization in humans," *Neurosci Lett*, vol. 331, no. 1, pp. 29–32, 2002.
- [6] L. Leocani, et al., "Event-related coherence and event-related desynchronization/synchronization in the 10 Hz and 20 Hz EEG during self-paced movements," *Electroencephalogr Clin Neurophys*, vol. 104, no. 3, pp. 199–206, 1997.
- [7] S. Ohara, et al., "Movement-related change of electrocorticographic activity in human supplementary motor area proper," *Brain*, vol. 123, no. 6, pp. 1203–1215, 2000.
- [8] G. Pfurtscheller and C. Neuper, "Simultaneous EEG 10 Hz desynchronization and 40 Hz synchronization during finger movements," *Neuroreport*, vol. 3, pp. 1057–1060, 1992.
- [9] C. Toro, et al., "Event-related desynchronization and movement-related cortical potentials on the ECoG and EEG," *Electroencephalogr Clin Neurophys*, vol. 93, pp. 380–389, 1994.
- [10] S. V. Sarma, et al., "Using point process models to compare neuronal activity in sub-thalamic nucleus of parkinson's patients and a healthy primate," *IEEE Trans Biomed Eng*, vol. 57, pp. 1297–1305, 2010.
- [11] J. N. Sanes and J. P. Donoghue, "Oscillations in local field potentials of the primate motor cortex during voluntary movement," *Proc Natl Acad Sci U S A*, vol. 90, p. 44704474, 1993.
- [12] V. N. Murthy and E. E. Fetz, "Oscillatory activity in sensorimotor cortex of awake monkeys: synchronization of local field potentials and relation to behavior," *J Neurophys*, vol. 76, no. 6, pp. 3949–3967, 1996.
- [13] J. P. Donoghue, et al., "Neural discharge and local field potential oscillations in primate motor cortex during voluntary movements," *J Neurophys*, vol. 79, no. 1, pp. 159–173, 1998.
- [14] A. Georgopoulos, et al., "On the relations between the direction of two-dimensional arm movements and cell discharge in primate motor cortex," *J Neurosci*, vol. 2, no. 11, pp. 1527–1537, 1982.
- [15] R. E. Kass and V. Ventura, "A spike train probability model," *Neural Comput*, vol. 13, pp. 1713–1720, 2001.
- [16] W. Truccolo, et al., "A point process framework for relating neural spiking activity for spiking history, neural ensemble and extrinsic covariate effects," *J Neurophys*, vol. 93, pp. 1074–1089, 2005.
- [17] L. Paninski, "Maximum likelihood estimation of cascade point-process neural encoding models," *Network: Comp in Neural Sys*, vol. 15(4), pp. 243–262, 2004.
- [18] D. L. Snyder and M. I. Miller, *Random Point Processes in Time and Space*. New York, NY: Springer, 1991.
- [19] E. N. Brown, et al., "Likelihood methods of neural data analysis," in *Computational Neuroscience (Feng, J.)*. London: CRC, 2003, ch. 9, pp. 253–286.
- [20] P. McCullagh and J. A. Nelder, *Generalized Linear Models*, 2nd ed. Boca Raton, FL: Chapman & Hall / CRC, 1989.
- [21] G. Czanner, et al., "Analysis of between-trial and within-trial neural spiking dynamics," *J Neurophys*, vol. 99, pp. 2672–2693, 2008.